Supplemental Information

pH-manipulated large-scale synthesis of $Na_3(VOPO_4)_2F$ at low temperature for practical application in sodium ion batteries

Lianjie Li[a,b,#], Junjie Fan[a,b,#], Hao Chen[a,b], Hui Liu[a,b], Qiulin Li[a,b], Changpeng Xian[a,b], Jin Wu[a,b], Yuruo Qi[a,b,*], Maowen Xu[a,b,*]

L. J. Li, J. J. Fan, H. Chen, H. Liu, Q. L. Li, C. P. Xian, J. Wu, Prof. Y. R. Qi, Prof. M. W. Xu

[a] School of Materials and Energy, Southwest University, Chongqing, 400715, PR China

[b] Chongqing Key Lab for Advanced Materials and Clean Energies of Technologies, Southwest University, Chongqing, 400715, PR China

[#] These authors contributed equally to this work.

*Corresponding author.

E-mail: xumaowen@swu.edu.cn (Prof. M.W. Xu); qiyuruojy@swu.edu.cn (Prof. Y. R. Qi)

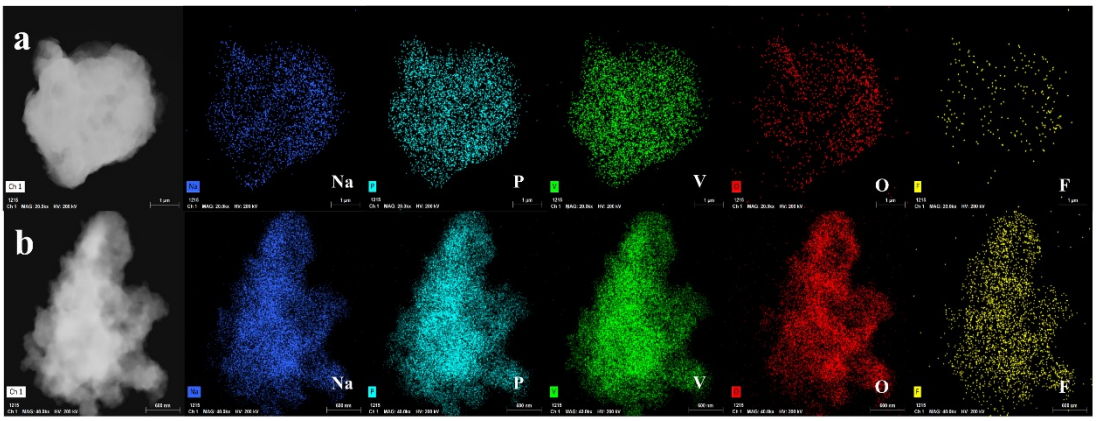

Figure S1 TEM-EDX elements mapping of C1(a) and C3 (b)

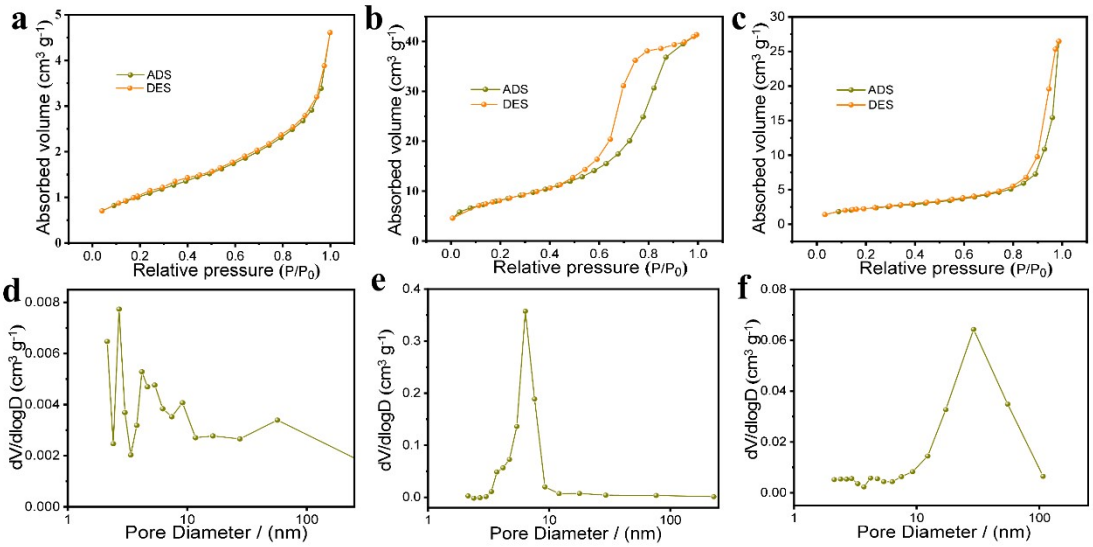

Figure S2 Nitrogen adsorption/desorption isotherms and pore diameter distribution of C1 (a,d), C2 (b,e), and C3 (c,f)

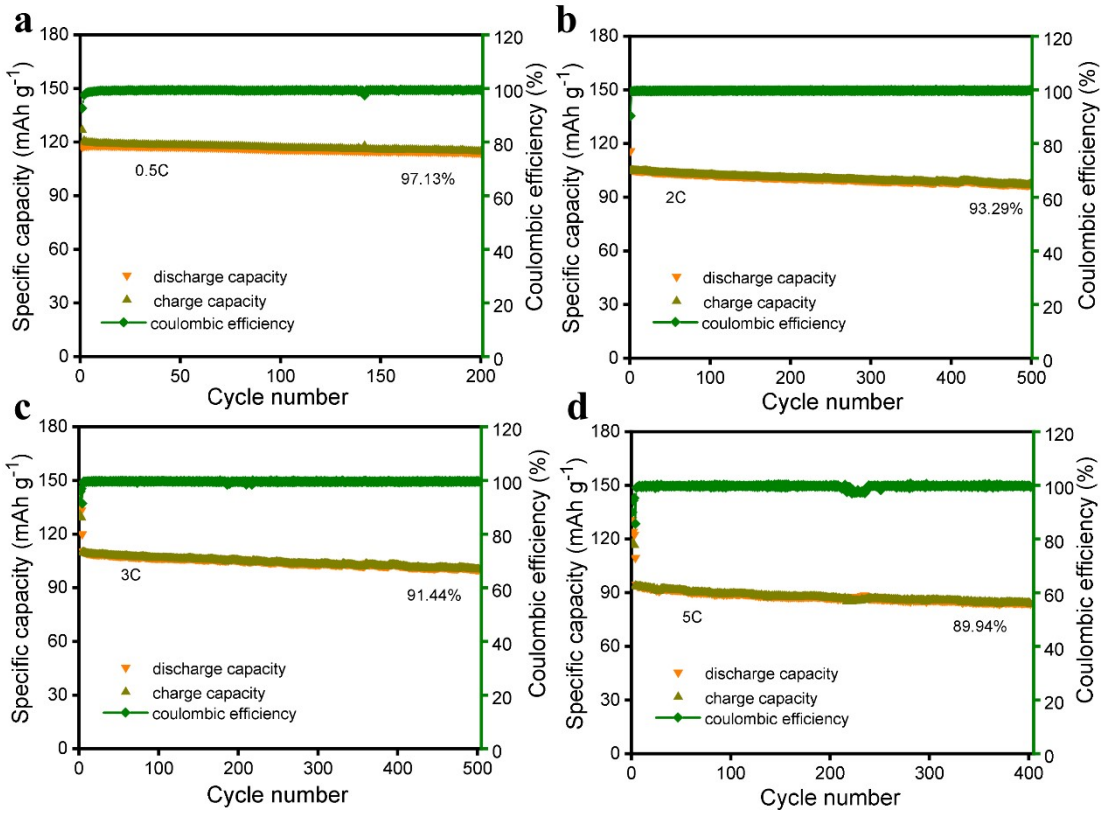

Figure S3 Cycling performance of C2 at 0.5, 2C,3C,and 5C currents rates, respectively.

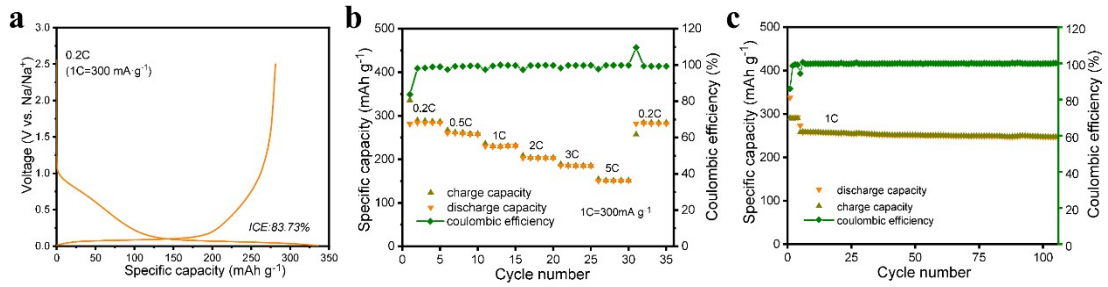

Figure S4 (a) First cycle charge/discharge curve of HC (b) The rate capability of HC electrode at various rates from C/5 to 5 C (c) The cycling performance of HC electrode at a current rate of 1C

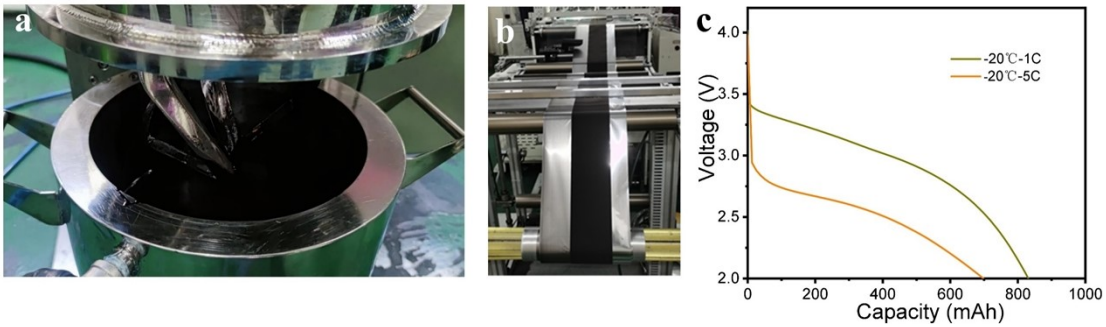

Figure S5 NVOPF soft-pack battery. (a) NVOPF electrode paste, (b) NVOPF sheet, (c) Discharge curves of soft-pack batteries at 1C and 5C at -20℃.

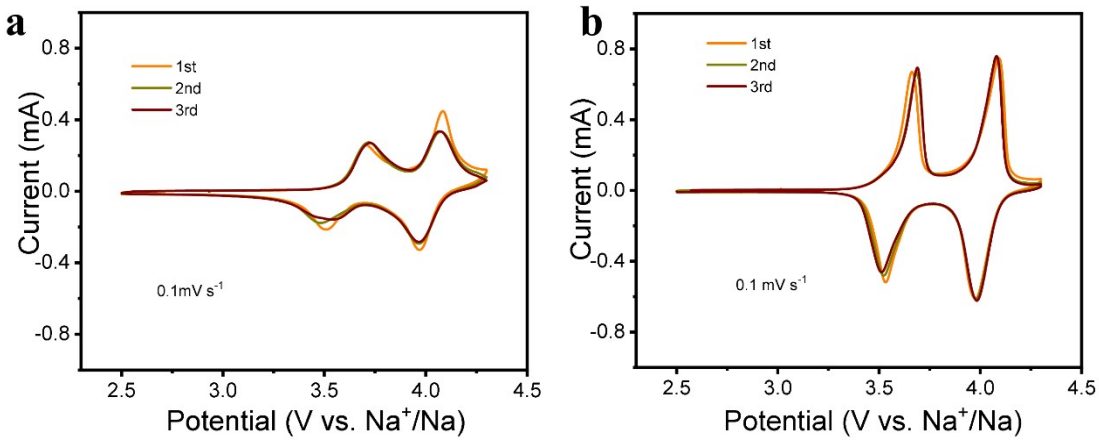

Figure S6 The CV curves of C1 (a) andC3 (b)

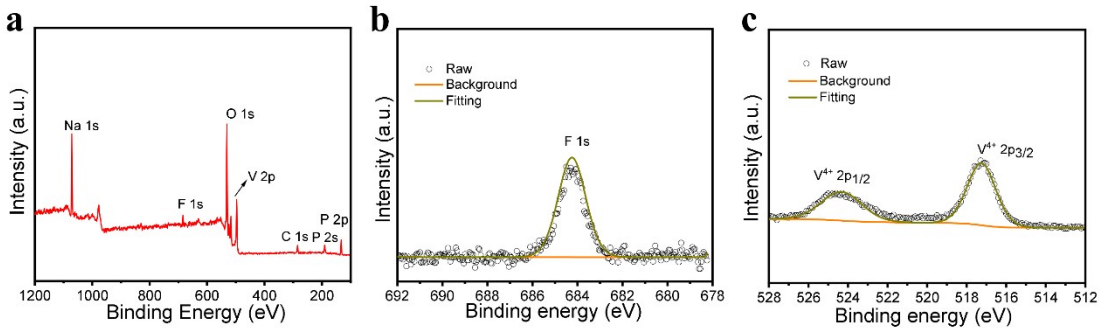

Figure S7 (a) The full spectra of C2 (b) F 1S XPS spectra (c) V 2p XPS spectra

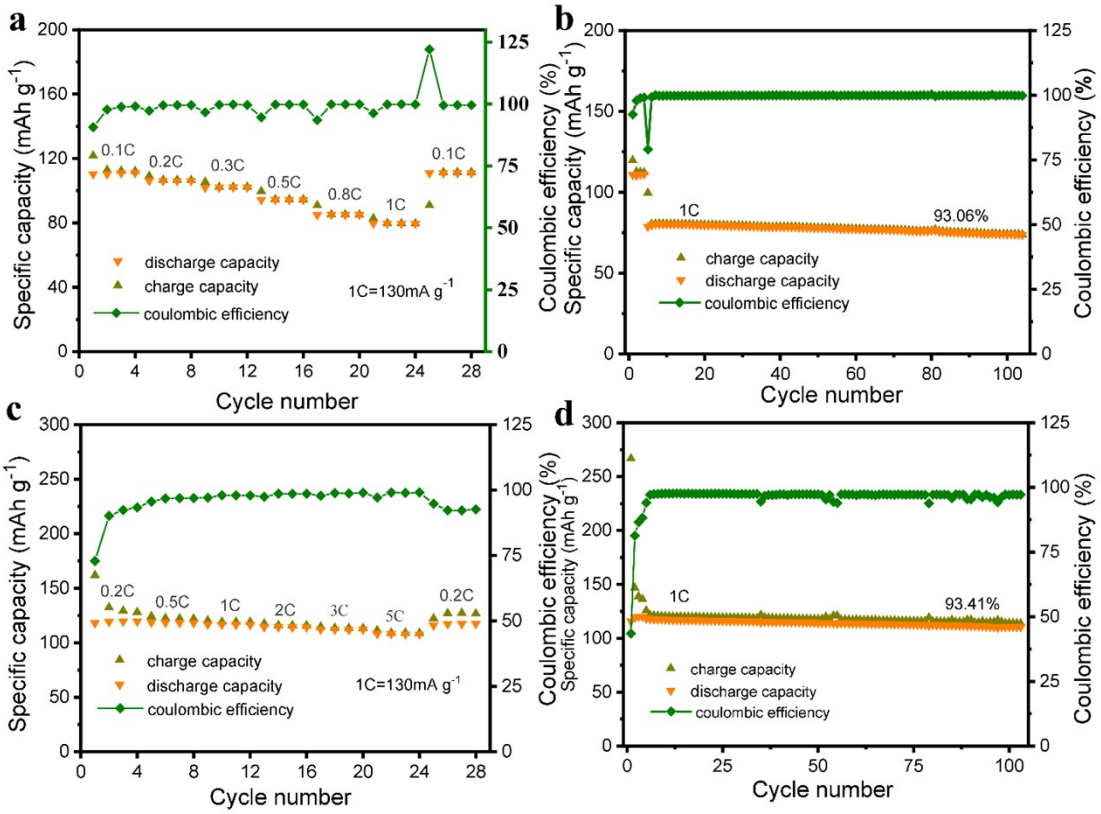

Figure S8 (a) The rate capability of C2 at -20℃ (b) The cycling performance of C2 at -20℃ (c) The rate capability of C2 at 50℃ (d) The cycling performance of C2 at 50℃

Table S1 Crystallographic and Rietveld refinement data of as-synthesized $Na_3(VOPO_4)_2F$.

Formula	$Na_3(VOPO_4)_2F$(C2)	
Space group	*I4/mmm* (139) - tetragonal	$P4_2/mnm$ (136) - tetragonal
Cell parameters	a = 6.3844Å	a = 9.0200 Å
	b = 6.3844Å	b = 9.0200Å
	c = 10.6644Å	c = 10.6421 Å
	$\alpha = \beta = \gamma = 90°$	$\alpha = \beta = \gamma = 90°$
	V = 434.68(2)Å^3, Z = 4	V = 865.84 (5)Å^3, Z = 6
Reliability factors	R_{wp} = 4.92%	R_{wp} =10.40%
	R_p = 3.73%	R_p = 7.59%
	χ^2 = 2.38	χ^2 = 6.68

Table S2 Results of ICP analysis

element	element concentration (mg/L)	element content (wt. %)	The average molar ratio of Na/V
Na	314.605	16.951	1.516:1
V	459.641	24.765	

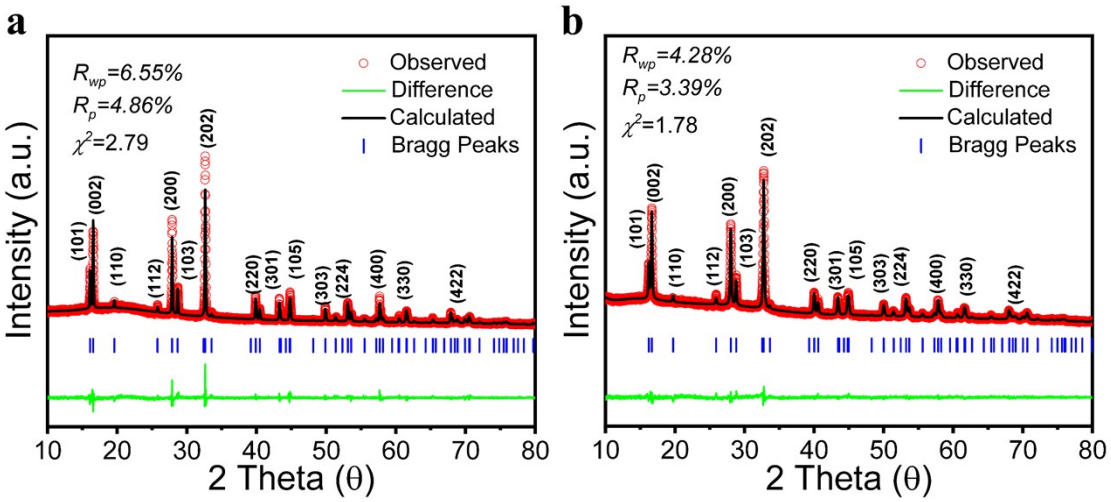

Figure S9 The XRD Rietveld refinement maps of C1(a) and C3(b).

As shown in **Fig. S9**, the *I4*/mmm space group is used for C1(a) and C3(b), and the fitted data agree in accordance with the experimental data. C1(a) has an R_{wp} of 6.55% and an R_p of 4.86%, while C3(b) has an R_{wp} of 4.28% and an R_p of 3.39%.

Table S3 Crystallographic and Rietveld refinement data of all samples

Formula	$Na_3(VOPO_4)_2F$(C1)	$Na_3(VOPO_4)_2F$(C2)	$Na_3(VOPO_4)_2F$(C3)
Space group	*I4/mmm* (139) - tetragonal		
Cell parameters	a = 6.3782Å	a = 6.3844Å	a = 6.3783Å
	b = 6.3782Å	b = 6.3844Å	b = 6.3783Å
	c = 10.6476Å	c = 10.6644Å	c = 10.6635Å
	$\alpha = \beta = \gamma = 90°$	$\alpha = \beta = \gamma = 90°$	$\alpha = \beta = \gamma = 90°$
	V = 433.15(4)Å^3, Z = 4	V = 434.68(2)Å^3, Z = 4	V = 433.93(5)Å^3, Z = 4
Reliability factors	R_{wp} = 6.55%	R_{wp} = 4.92%	R_{wp} = 4.28%
	R_p = 4.86%	R_p = 3.73%	R_p = 3.39%
	χ^2 = 2.79	χ^2 = 2.38	χ^2 = 1.78

Table S4 Atomic coordinates, cation and anion occupancies of all samples

sample	atom	x	y	z	occupancy	U_{iso}
$Na_3(VOPO_4)_2F$ (C1)	Na1	0.27260	0.27260	0	0.6875	0.0293
	Na2	0.24408	0.5	0	0.0625	0.0664
	V	0	0	0.19918	1	0.0230
	P	0	0.5	0.25	1	0.0065
	O1	0	0.31455	0.16563	1	0.0113
	O2	0	0	0.35570	1	0.0163
	F	0	00	0	1	0.0184
$Na_3(VOPO_4)_2F$(C2)	Na1	0.27494	0.27494	0	0.6875	0.0298
	Na2	0.2357	0.5	0	0.0625	0.0612
	V	0	0	0.20026	1	0.0207
	P	0	0.5	0.25	1	0.0070
	O1	0	0.31363	0.16492	1	0.0077
	O2	0	0	0.35615	1	0.0184
	F	0	0	0	1	0.0176
$Na_3(VOPO_4)_2F$(C3)	Na1	0.27452	0.27452	0	0.6875	0.0271
	Na2	0.24524	0.5	0	0.0625	0.0642
	V	0	0	0.19925	1	0.0254
	P	0	0.5	0.25	1	0.0038
	O1	0	0.315118	0.16571	1	0.0108
	O2	0	0	0.35591	1	0.0084
	F	0	0	0	1	0.0150

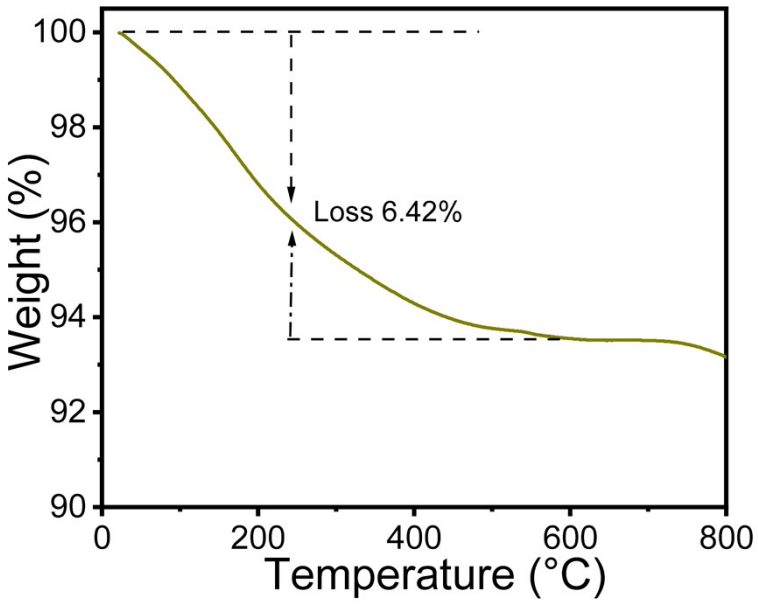

Figure S10 The TGA curve of the NVOPF

We have experimented with carbon coating the material with organic carbon sources $C_6H_{12}O_6$, NVOPF and $C_6H_{12}O_6$ were mixed well and transferred to a tube furnace at 350°C for 4h and 500°C(550℃) for 8h to obtain NVOPF@500℃ and NVOPF@550℃. It should be noted that $C_6H_{12}O_6$ was added at 5% of the mass of NVOPF. The XRD curve was shown in **Fig. S11**, especially, **Fig. S11b** is a partial enlargement of **Fig. S11a** from 12° to 38°.

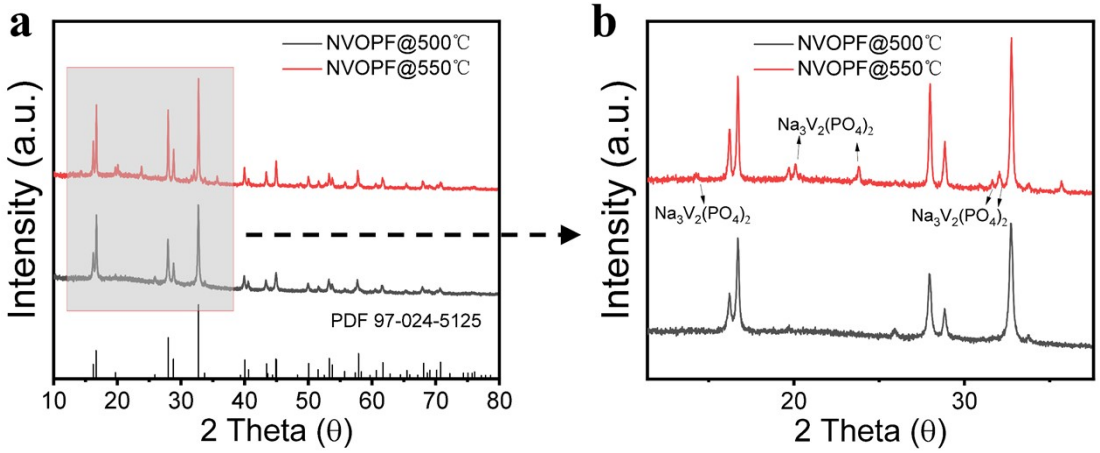

Figure S11 the XRD pattern of NVOPF@500℃ and NVOPF@550℃

As shown in **Fig. S11**， The XRD peaks at a heating temperature of 500°C are more consistent with the NVOPF PDF (97-024-5125) card. At 550°C, the heterogeneous phase $Na_3V_2(PO_4)_{3(}$NVP) appears due to the loss of fluoride ions at higher temperatures. Furthermore，The difference between $Na_3(VPO_4)_2F_3$(NVPF)and $Na_3(VOPO_4)_2F$(NVOPF) is that the V in NVOPF is V^{4+} instead of V^{3+}. V^{4+} is more easily reduced to V^{3+} at high temperatures. Additionally, the loss of fluoride ions at high temperatures leads to the generation of heterogeneous phases of (NVP) more readily[1]. This is the reason why many sol-gel methods produce heterogeneous phases of NVP. High-temperature solid phase methods face the same problem as they are subjected to long periods of high-temperature treatment[2].

Fig. S12a presents the first charge/discharge curves at a current rate of 0.2C (corresponding to a current density of 26 mA g^{-1}). Two samples reveal two charge/discharge plateaus at approximately 3.6 V and 4.0 V. Furthermore,

NVOPF@550°C shows an additional plateau at 3.4V. It should be noted that there is a significant voltage drop at approximately 3.5V during the discharge of NVOPF@500℃. This voltage drop is primarily caused by the continuing reaction between the sodium layer and the electrolyte, so the polarization of the passivation layer on the surface of the sodium increases, and the sodium requires more energy to dissolve, which is not related to the positive electrode[3]. In addition, rate performance tests were conducted at different current rates of 0.2C, 0.5C, 1C, 2C, 3C, and 5C (**Fig. S12b**). The capacity retention at 5C for two samples are 54.44%(NVOPF@500℃), 68.86%(NVOPF@550℃), respectively. When returns to 0.2C after 30 cycles, the capacity loss of three samples is 0.63%, and 5.33%, respectively. The cycling performance of the two samples is compared in **Fig.S12c**. Over the long span of 400 cycles at 1C, the capacity retention of NVOPF@500℃ is 97.25%, while the NVOPF@550℃ is 86.32% after 120 cycles. It is better to use a highly conductive composite conductive agent instead of carbon coating(a high discharge capacity of 119.6 mA h g^{-1} at 0.2C and remarkable cycling performance with a capacity retention of approximately 94.0% after 1400 cycles at 1C).

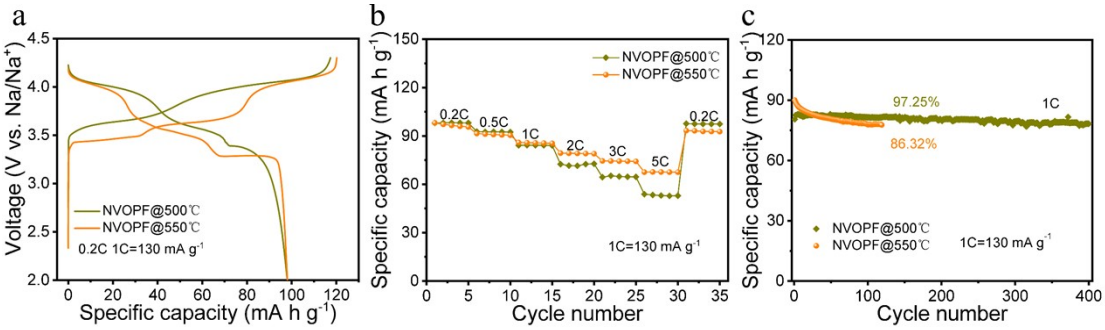

Figure S12 The electrochemical performance of carbon coating. (a) Charge/discharge curves in the first cycle; (b) Rate capability;(c) Cycling performance at 1C.

As temperature and time increase, the 3.4 V platform of the impurity NVP becomes longer, while the 3.6 V and 4.0 V platforms of the main phase NVOPF become shorter. This is evidenced by the gradual weakening of the characteristic peaks of the main-phase NVOPF in XRD and the increasing strength of the characteristic peaks of the impurity NVP. Eventually, The NVOPF main phase transforms an impurity NVP.

Although impurity NVP does not appear after heat treatment at 500°C, the graphitization of the carbon layer may be low due to the low heat treatment temperature of the carbon cladding. This can result in poor conductivity, which can negatively affect the electrochemical performance.

In conclusion, considering both production cost and performance, the preparation of pastes may benefit from the use of highly conductive composite conductors, such as KB+CNT.

[1] L. Deng, F.-D. Yu, Y. Xia, Y.-S. Jiang, X.-L. Sui, L. Zhao, X.-H. Meng, L.-F. Que and Z.-B. Wang, Stabilizing fluorine to achieve high-voltage and ultra-stable Na3V2(PO4)2F3 cathode for sodium ion batteries, *Nano Energy*, 2021, **82**, 105659.

[2] M. Wang, X. Huang, H. Wang, T. Zhou, H. Xie and Y. Ren, Synthesis and electrochemical performances of $Na_3V_2(PO_4)_2F_3$/C composites as cathode materials for sodium ion batteries, *RSC Adv.*, 2019, **9**, 30628–30636.

[3] A. Rudola, D. Aurbach and P. Balaya, A new phenomenon in sodium batteries: Voltage step due to solvent interaction, *Electrochemistry Communications*, 2014, **46**, 56–59.